Dalton Transactions

Accepted Manuscript

ROYAL SOCIETY OF CHEMISTRY

www.rsc.org/dalton

Structures and Photophysical Properties of Copper(I) Complexes Bearing Diphenylphenanthroline and Bis(diphenylphosphino)alkane: The Effect of Phenyl Groups on the Phenanthroline Ligand

Taro Tsubomura,[a*] Kaoru Kimura,[a] Michihiro Nishikawa, [a] and Toshiaki Tsukuda[b]

[a] Department of Materials and Life Science, Seikei University, Musashino Tokyo, Japan

[b] Faculty of Education and Human Science, University of Yamanashi, Kofu, Yamanashi, Japan

Abstract

A series of copper(I) complexes bearing 2,9-dimethyl-4,7-diphenyl-1,10-phenanthroline (dmpp) and a diphosphine ligand have been prepared. The diphosphine ligands used have two, three or four methylene carbons between the two phosphorous atoms. The crystallographic study has revealed that two of the three complexes have the mononuclear structure bearing dmpp and a bidentate diphosphine ligand, and one is a diphosphine-bridged binuclear complex. The photoluminescence of the complexes in solution was studied and compared with the previously reported complexes bearing 2,9-dimethyl-1,10- phenanthroline (dmp). It was found that the two phenyl groups on the phenanthroline ligand have a marked effect on the photophysical properties of the complexes; the intensity of the emission of the complexes is greatly enhanced by the phenyl groups. The photophysics of the complexes are discussed with the results of DFT and TDDFT calculation.

Introduction

Luminescence of copper(I) complexes have attracted a special interest due to potential applications for OLED,[1] solar cell,[2,3] sensor,[4,5] and photochemical reactions.[6,7] A lot of copper(I) emitters have been proposed in the past decade; they include bis(phenanthroline) type complexes, amidophosphine complexes,[8,9] binuclear phosphine complexes[10–13], carbene complexes[14,15] and neutral complexes bearing modified diimine type ligands.[16,17] One of the most intensively studied types of the complexes is the copper(I) species having a 2,9-disubstituted 1,10-phenanthroline ligand and a diphosphine ligand.[18] We previously reported a series of copper complexes (**1a**, **2a**, and **3a** shown in scheme 1) bearing dmp (= 2,9-dimethyl-1,10-phenanthlorine) and a diphosphine ligand.[19] Armaroli et al. reported that a complex $[Cu(dmpp)(DPEphos)]^+$, where dmpp and DPEphos are 2,9-dimethyl-4,7-diphenyl-1,10-phenanthroline and 2,2'-Bis(diphenylphosphino)diphenyl ether, respectively, shows high-quantum yield luminescence in solution.[20] Introduction of two phenyl groups into the phenanthroline ligand seems to be effective to increase the quantum yield of the luminescence of copper(I) complexes. Xu et al. also showed some dmpp complexes could be used as an efficient emitter in photodetector devises.[21]

We found that the emission quantum yields increase with the length of the methylene chain between the two phosphorus donor atoms.[19] In the series of the complexes, **1a** – **3a**, the quantum yield of **3a** is highest, and **3a** only has the binuclear structure in which the diphosphine ligand, dppb, acts as a bridging ligand. The unique photophysical properties of **3a** as a strong emitter rely on the binuclear structure, and the mechanism of the emission should be important for developing promising photofunctional materials. In this study, we prepared a new series of the copper(I) complexes (**1b**, **2b**, and **3b**) bearing dmpp and a diphosphine ligands, dppe (1,2-bis(diphenylphosphino)ethane), dppp (1,3-bis(diphenylphosphino)propane), or dppb (1,4-bis(diphenylphosphino)butane). The structure and photophysics of the new complexes have been compared with the previously reported complexes (**1a**, **2a**, and **3a**). To our best of knowledge, no paper has discussed the effect of the phenyl group on 2,9-dimethyl-1,10-phenanthroline systematically. We examined the effects in detail performing both experimental and theoretical studies for the complexes.

Experimental

The salt, tetrakis(acetonitrile)copper(I) hexafluorophosphate,[22] was prepared according to the literature. All ligands were obtained from commercial suppliers and used without further purification. ^{1}H-NMR spectra were recorded on a JEOL Delta-500 spectrometer using TMS as an internal standard. Absorption and emission spectra were obtained in a solvent degassed by at least five freeze-pump-thaw cycles using a quartz cell fitted with a Teflon vacuum stop cock. Absorption spectra were measured on a Shimadzu UV-3000 spectrometer and an Agilent 8453 spectrometer. Emission spectra and emission lifetimes were collected on a laboratory-made apparatus. Briefly, the samples were excited by a monochromated Xenon light source and the emission was analyzed by a cooled CCD spectrometer. For the lifetime measurement,

a nitrogen laser was used to excite the samples, and the emission was detected by a monochromator equipped with a photomultiplier tube, and the signal was analyzed by a digital oscilloscope. Details of the luminescence measurements were described in the previous paper.[23] Emission quantum yields in solution were determined using $[Ru(bpy)_3]Cl_2$ in acetonitrile solution as a standard (Φ = 9.4%).[24]

X-ray crystallography.

X-ray crystallographic measurements of the three complexes were made on a Rigaku Saturn 70 CCD area detector with graphite-monochromated MoKα radiation. The crystal-to-detector distance was 54.9 mm. The data were collected with maximum 2θ value of 55.0^{o}. The data were processed by using the *CrystalClear* software.[25a] Absorption corrections were made by the numerical method. The structures were solved by direct methods (SIR-2004[25b] for **1b** and **2b**, SIR-92[25c] for **3b**) and refined by the full matrix least squares procedures (SHELXL-97).[25d] The non-hydrogen atoms are refined with anisotropic temperature factors and the positions of all hydrogen atoms were calculated using the riding model. All calculations were performed by using the CrystalStructure or Wingx[25e] crystallographic software package. For **2b**, the SQUEEZ software[25f] showed there are 1235 Å^3 void and suggested 192 electrons in the void. Therefore, two diethyl ether molecules were assumed to be in the void. Using a new data set of the structure factors calculated by the software, an additional least-squares calculation gave the final result.

Crystallographic data have been deposited with Cambridge Crystallographic Data Centre: Deposition number CCDC 976959, 976958, and 993068 for **1b**, **2b**, and **3b**, respectively. Copies of the data can be obtained free of charge via http://www.ccdc.cam.ac.uk/conts/retrieving.html (or from the Cambridge Crystallographic Data Centre, 12, Union Road, Cambridge, CB2 1EZ, UK; Fax: +44 1223 336033; e-mail: deposit@ccdc.cam.ac.uk).

Syntheses of the copper(I) complexes.

$[Cu(dmpp)(dppe)]PF_6$ (**1b**$\cdot$ PF_6). The solvents used in the synthesis were degassed by bubbling argon gas. In a Schrenk tube, tetakis(acetonitrile)copper(I) hexafluorophosphate (0.25 mmol) was added to the dichloromethane solution (5 mL) containing dppe (0.25 mmol) and dmpp (0.25 mmol). The solution was stirred for 1 h at room temperature, and then 5 ml of diethyl ether was slowly added to the solution. The mixture was kept in a refrigerator overnight. Orange precipitates were obtained by filtration (yield, 18%). The product was stable in air. Anal. Found: C, 63.97; H. 4.24; N, 2.45. Calcd. for $CuC_{52}H_{44}N_2P_2\cdot PF_6\cdot 0.2(CH_2Cl_2)$: C, 63.69; H, 4.55, N, 2.85. ^{1}H NMR ($CDCl_3$) : δ 8.08 (s, 2H, dmpp C*H*), 7.64-7.56 (m, 12H, dmpp C*H*, C_6H_5), 7.4-7.2 (m, 20H, dppe C*H*), 3.10 (m, 4H, CH_2), 2.10 (s, 6H, CH_3). Other heteroleptic compounds were prepared in a similar manner.

$[Cu(dmpp)(dppp)]PF_6$ (**2b**$\cdot$ PF_6). Yellow powders (yield, 33%). Anal. Found: C, 64.59; H. 4.66; N, 2.65. Calcd. for $CuC_{53}H_{46}N_2P_2\cdot PF_6$: C, 64.86; H, 4.72, N, 2.85. ^{1}H NMR ($CDCl_3$) : δ 8.07 (s, 2H, dmpp C*H*), 7.65-7.55 (m, 10H, dmpp C_6H_5), 7.52 (s, 2H, dmpp. C*H*), 7.3-7.1 (m, 20H, dppp C*H*), 2.88 (m, 4H, CH_2), 2.78-2.63 (m, 2H, CH_2), 2.20 (s, 6H, CH_3).

$[Cu_2(dmpp)_2(dppb)_2](PF_6)_2$ (**3b**·$(PF_6)_2$). Yellow powders (yield, 67%). Anal. Found: C, 64.44; H. 4.76; N, 2.57. Calcd. for $Cu_2C_{108}H_{96}N_4P_4 \cdot 2(PF_6) \cdot 0.2(CH_2Cl_2)$: C, 64.72; H, 4.84, N, 2.79. ^{1}H NMR ($CDCl_3$) : δ 8.02 (s, 2H, dmpp C*H*), 7.62-7.54 (m, 10H, dmpp C_6H_5), 7.42 (s, 2H, dmpp C*H*), 7.3-7.1 (m, 20H, dppb C*H*), 2.82 (m br, 4H, CH_2), 2.35 (m, 4H, CH_2), 2.23 (s, 6H, CH_3).

Quantum chemical calculations.

DFT and TDDFT calculations were done using Gaussian 03 and 09 software[26] using b3lyp functional. Basis sets are as follows; Cu, 6-311G with Wachters's 4p functions,[27] phosphorus and nitrogen 6-31G*+, carbon 6-31G*, and hydrogen 6-31G. Structure optimization of the singlet ground states have been performed by DFT calculations. Then, TDDFT calculations of the singlet and triplet excited states were done using the optimized geometry. Orbital pictures were generated by Molekel software.[28] Mulliken population analysis were performed by AOMix software.[29] Detailed examination of TDDFT results was done using Multifwn software.[30]

Results and Discussion

Synthesis and structures

The preparation of the heteroleptic copper(I) complexes containing diphosphine and diimine ligands is straightforward and is schematically illustrated in the scheme 1. The complex, tetrakis(acetonitrile)copper(I) hexafluorophosphate, was used as a starting material, and the heteroleptic complexes have been obtained as PF_6^- salts. The solids are all stable in air and can be stored for long term. They were identified by CHN elemental analyses, NMR (Fig. S1-S9) and X-ray diffraction studies. It should be noted that mononuclear complexes are solely obtained using dppe or dppp as the diphosphine ligands, but the dinuclear complex was only isolated for the dppb complex.

The structures of the new three complexes were analyzed by single crystal X-ray diffraction studies. The crystal data for **1b**, **2b**, and **3b** are tabulated in Table S1, the structures are shown in Fig. 1, and the geometrical parameters around the copper atoms are listed in Table 1. The complexes **1b** and **2b** have a distorted tetrahedral structure. **3b** is a dinuclear complex, in which two dppb ligands bridge the two copper(I) atoms. Two phosphorous atoms of the dppb ligands and two nitrogen atoms of a dmpp chelate bind to each copper(I) atom. Coordination geometry around each copper(I) center in **3b** is also distorted tetrahedral. Therefore, the geometries around the copper atoms are similar (N_2P_2 coordination) for the three complexes. An inversion center lies on the center of the complexes. The bond lengths, Cu-N and Cu-P, are 2.02 – 2.13 Å and 2.23 – 2.29 Å, respectively, which are moderate values for a family of copper(I) complexes bearing diimine and diphosphine ligands.[31] The bite angles, N-Cu-N, are similar and in the range 82-80° for the three complexes, but the angles P-Cu-P are 91°, 105° and 120°, respectively for **1b**, **2b**, and **3b**. We previously showed that the P-Cu-P angle is very important factor for the photophysical

properties of the complexes.[19] The P-Cu-P angle for the complex **3b**, which is smaller than that of **3a** (126°), but it is far larger than the bite angles observed in **1b** and **2b**. The large bite angles of **3a** and **3b** are mainly due to the steric reason; two methylene chains in the dppb ligands are oriented in parallel, and the interligand CH· · · HC contacts (2.28 Å) are near the sum of the van der Waals radius of hydrogen atom (see Fig. S12). The dihedral angles between the two planes which are defined by three atoms, N1, Cu1, N2 and P1, Cu1, P2 in **1b**, **2b**, and **3b** are 85.5°, 87.5°, and 89.0°, respectively. The angles describe the degree of the flattening distortion, which are 90° in the idealized tetrahedral geometry. The angles are not so much deviated from that in the dmp complexes, **1a** (89.5° and 87.2° for the two independent complex cations in the unit cell), **2a** (86.2° and 83.8°), and **3a** (86.5°). The rocking angles, X-Cu-Y, in which X and Y are the midpoints between the two nitrogen atoms and two phosphorous atoms, respectively, are 4.9°, 4.3°, and 6.2° for **1b**, **2b**, and **3b**, respectively. The values show that the rocking is small in the crystal. The dihedral angles between the mean plane of phenanthroline ring and the phenyl group on the N1 and N2 side, β_1 and β_2, are 50-64° in **1b**, **2b**, and **3b** (Table 1), suggesting that the there are no obvious π-conjugation between the phenanthroline moiety and the phenyl groups; the role of the groups will be discussed in the later section.

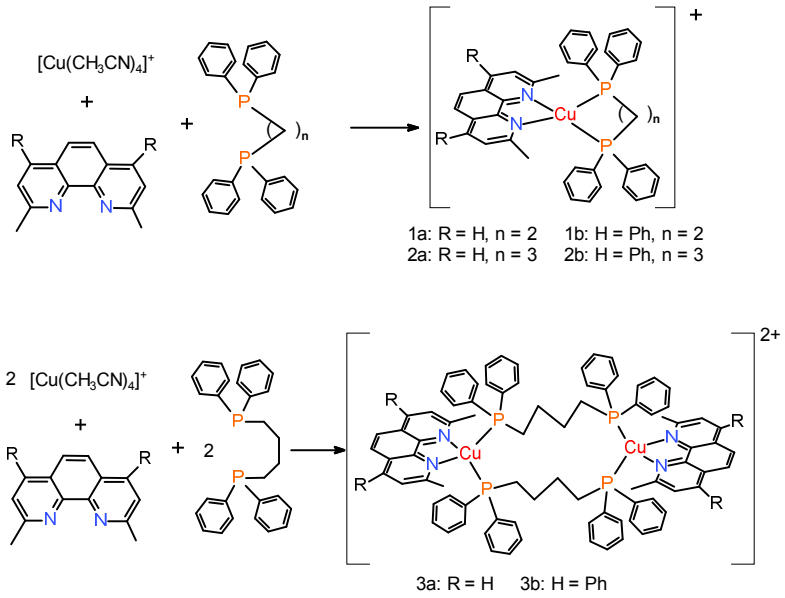

Scheme 1

We should keep in mind the possibility of the disproportionation reaction of the heteroleptic complexes, $[Cu(P\text{^}P)(N\text{^}N)]^+$, into $[Cu(P\text{^}P)_2]^+$ and $[Cu(N\text{^}N)_2]^+$ in solution.[32] ^{1}H NMR showed that, in sufficiently diluted (< 1 mM) $CDCl_3$ solution of the heteroleptic complexes, the amount of bis(dmpp)copper(I) ion was negligible immediately after dissolution of the heteroleptic complexes (Fig. S1, S4, S7). The homoleptic species made by the disproportionation were detected in the same solution kept in the dark at room temperature for 4 days (Fig. S2, S5, S8). The ratio of the species made by disproportionation of **3b** is much

smaller than those of **1b** and **2b**. The disproportionation in higher concentration (> 10 mM) was observed even immediately after the dissolution of the samples (Fig. S3, S6, S9), probably because the disproportionation reaction is much faster than that in low concentration; the color of the solution obviously changed from yellow, which is characteristic of heteroleptic complex, to red, which is characteristic of bis(dmpp)copper(I) complex, during NMR measurements. However, under the conditions where spectroscopic measurement has been performed (< 10^{-4}M), the reaction seems to be sufficiently slow to study the properties of the complexes. We also check the absorption around 470 nm, which is characteristic of bis(diimine)copper(I) complexes, of sufficiently diluted **3b** in degassed dichloromethane at room temperature in the dark, which are the same conditions as those for photophysical measurements, is negligible 5 hours after dissolving the solid sample (Fig. S10). Therefore, we concluded that the products of the disproportionation reaction should be negligible if the spectral measurements of the dilute solution of the heteroleptic complexes were performed as soon as possible after dissolution of the samples.

Photophysical properties

The absorption spectra of the complexes in dichloromethane solution are presented in Fig. 2. The absorption data are listed in Table 2. The complexes **1b**, **2b**, and **3b** have absorption bands with moderate intensity (ε = 4500 – 6200 M^{-1} cm^{-1}) at about 400 nm. Very interesting trends are found in the absorption bands. 1) Gradual blue shifts were observed as the number of carbon atoms increases between the two phosphine atoms. 2) The absorption energy of the complexes does not largely depend on the diimine ligands. Small red shifts are observed if the diimine ligands are changed from dmp to dmpp for all three diphosphine ligands. 3) The absorption intensity of the dmpp complexes is much larger than those of the corresponding dmp complex; 3200→6200, 3200→5900, and 2800→ 5000 $M^{-1}cm^{-1}$, respectively for dppe, dppp, and dppb complexes. The relationship between the bite angles of the diphosphine chelate and the absorption energies was observed not only in the previously reported dmp complexes[19] but also in the dmpp complexes.

The emission spectra are shown in Fig. 3. Interestingly, the wavelength of the emission maxima of the three complexes, **1b**, **2b**, and **3b** gradually decrease by 20 nm as the number of methylene chains increases, the results are in accordance with that of the absorption spectra (Table 2). The quantum yields (Φ) of **1b**, **2b**, and **3b** in degassed dichloromethane are 1.7%, 6.6%, and 16%, respectively. The value of **3b** is relatively high as that of copper(I) complex observed in solution. The lifetimes (τ) of **1b**, **2b**, and **3b** under the same conditions are 1.2 μs, 4.4 μs, and 10.0 μs, respectively. One can see an interesting trend in the data shown in Table 2 that the quantum yields of the complexes are enhanced if the diimine ligand is changed from dmp to dmpp for each diphosphine complex, but the lifetimes do not basically depend on the diimine ligand.

We now compare the luminescent properties of the complexes in terms of the radiative and non-radiative rate constants. In the following discussion, we use the "observed" rate constants, k_r and k_{nr}, which are defined as $k_r = \Phi / \tau$ and $k_{nr} = (1 - \Phi) / \tau$. It is well known that the emission of many copper(I) complexes are actually delayed fluorescence emitted from the thermally activated singlet state. The

observed radiative rate constants represent the weighted average of the rate constants of the two emitting process, fluorescence and phosphorescence.[33]

As for the difference in the in the complexes **1b**, **2b**, and **3b**, we already reported a similar trend in the photophysics of the three complexes **1a**, **2a**, and **3a**; the extension of the methylene chains in the diphosphine ligands leads to the increase in the emission quantum yields of the complexes.[19] The analysis on the photophysical data for **1a**, **2a**, and **3a** showed that the increase in the quantum yields was explicitly due to the reduction of the non-radiative radiation rates. The radiative rate constants for the three complexes were essentially the same. For the present three complexes, **1b**, **2b**, and **3b**, the same trends have been observed for the rate constants. The constants, k_rs, for the three complexes are similar and they are 1.4×10^4, 1.5×10^4 and 1.6×10^4 s^{-1}, respectively for **1b**, **2b**, and **3b**. On the other hand, k_{nr}s greatly depend on the diphosphine ligands; 8.0×10^5, 2.3×10^5 and 1.0×10^5 s^{-1}, respectively for **1b**, **2b**, and **3b**. Therefore, the difference in the quantum yields of the three complexes was mainly determined by the rate of the non-radiative processes. As the number of methylene groups increases in the phosphine ligand, we observed smaller k_{nr}. The decrease in k_{nr} may be caused by two reasons; one is due to the energy-gap law. The emission energies of the complexes vary in the order **1b < 2b < 3b**, therefore the k_{nr}s should decrease in the order **1b > 2b > 3b**. The difference in the bite angles, P-Cu-P, should be another reason. The angle increases as the number of methylene carbons increases in the phosphine ligand. The large angle should reduce the flattening and rocking distortion in the excited states and inhibit the attack of the solvent molecule in the excited states, which are important quenching mechanisms in Cu(I) complexes.[34] The structure of **3b** shows two phenyl groups on the two phosphorous atoms are oriented to cover the Cu atoms (see Fig. 1 and Fig. S12); this may inhibit the access of solvent molecules to the metal centers. The Stokes-shift does not apparently depend on the number of methylene carbons; 8400 cm^{-1}, 8400 cm^{-1} and 8700 cm^{-1} for **1b**, **2b**, and **3b**, respectively; the result may show the decrease in k_{nr} in the complex having a longer phosphine ligand is mainly due to the blocking of the solvent access rather than the reduction of the distortion.

The difference in the luminescence between the dmp and dmpp complexes is remarkable. The quantum yields of the three dmpp complexes, **1b**, **2b**, and **3b,** are almost twice as large as the quantum yield of the dmp complexes, **1a**, **2a**, and **3a**, respectively. This is caused by the large k_rs of the dmpp complexes compared to those of dmp complexes as shown in Fig. 4.[35] On the other hand, k_{nr}s are almost independent of the diimine ligands. The result for the large radiative rates may be related to the large absorption coefficient of the ^{1}MLCT transition of the dmpp complexes compared to those of the dmp complexes as shown in the previous section. As stated above, the emission of the Cu(I) complexes are frequently thermally activated delayed fluorescence (TADF). Recently, it has been shown that the emission of many $[Cu(NN)(PP)]^+$ species is also TADF.[36] Large MLCT absorption intensity indicates that the radiative rate of the [^{1}MLCT $\rightarrow$ ground state] transition is fast, as a result, fast observed radiative rate should be observed. Therefore, the effect of the phenyl groups in the dmpp ligands on the emission can be explained by the enhancement of the ^{1}MLCT absorption intensity. Owing to the small k_{nr} and large k_r values, **3b** shows considerably strong emission in fluid solution at room temperature.

DFT and TDDFT calculations

As described above, two phenyl groups in the dmpp ligand have a pronounce effect on the photophysical properties of the Cu(I) complexes. The electronic structures of the complexes were studied by DFT and TDDFT calculations in order to explore the effect of two phenyl groups. A part of the results have been shown in Table 3, and the shapes of some Kohn-Sham orbitals have been depicted in Figure S11 in ESI. The following discussions are based on the results calculated with the optimized geometry in the singlet ground states of the complexes.

The composition of the K-S orbitals has been studied by Mulliken population analysis. The compositions of the frontier Kohn-Sham orbitals (from the HOMO-2 to LUMO+1) are similar for the complexes **1a**, **1b**, **2a** and **2b**, so the orbitals of the four complexes are discussed at the beginning of the discussion. For all complexes, HOMOs are constructed from the orbitals of copper (49 – 56%) and phosphorous atoms (30 – 39%) with a slight contribution of diimine moieties. In the HOMO-1 and HOMO-2, the copper atoms also have the largest contribution for the four complexes. The contribution of the diphosphine atoms to the HOMO-1 is very small, but there are considerable contributions of the phosphorous orbitals to the HOMO-2. The LUMO and LUMO+1 of the complexes can be regarded as diimine π* orbitals. The diphenyl moieties in the dmpp ligand are found to contribute to the frontier orbitals of **1b** and **2b**. The most considerable contribution of the two phenyl groups can be seen in the HOMO-3 orbitals. They are 20% and 31% for **1b** and **2b**, respectively. For the complexes **1a** and **2a**, the energy of the HOMO-3 is far low compared with the HOMO-2. However, for **1b** and **2b**, the energies of the HOMO-3 orbitals are similar to the HOMO-2 and there are considerable contributions of the diphenyl moieties to the HOMO-3, which should be marked contrast with those of **1a** and **2a**. The contribution of the two phenyl groups in the LUMO seems to be small; 7% and 8% for **1b** and **2b**, respectively. However, it was found that the electronic transitions are considerably affected by the apparently small contribution of the phenyl groups as revealed by the TDDFT calculation (vide infra).

For **3a** and **3b**, the calculation was performed under C_i symmetry. There are two chromophores in the two complexes, the interaction between them may be small; therefore, all orbitals are composed of pseudo degenerated pairs of orbitals having similar energy. The HOMO and HOMO-1 of **3a** and **3b** are essentially the same character with the HOMO of the other complexes, and the HOMO-2 and HOMO-3 of **3a** and **3b** are similar to the HOMO-1 of the other complexes, etc. It should be noted that in the dinuclear complexes, the HOMO-6 and HOMO-7 of **3b**, which correspond to the HOMO-3 of **1a**, **1b**, **2a** and **2b**, have considerable amplitude in the two phenyl groups. The orbitals, LUMO – LUMO+3, are mainly π* orbitals of the diimine ligands.

Table 4 shows that the lowest-energy singlet-singlet transitions of the mononuclear complexes are mainly composed of the HOMO → LUMO component for all complexes. For the dinuclear complexes, the HOMO–3 → LUMO, HOMO-2 → LUMO+1, and HOMO-1 → LUMO+1 terms also contribute to the transition. The result leads to a conclusion that the absorption bands observed at around 400 nm should be mainly attributed to the ^{1}MLCT (Cu(I) → diimine ligands) for all complexes.

The calculated wavelengths of the transitions are in the 400-450 nm range, which well agree with the observed values. As already discussed in the previous section, there are interesting trends in the absorption spectra of the complexes; i.e., 1) the wavelength of the absorption bands becomes shorter when the number of the carbon atoms between the phosphorous atoms in the phosphine ligand increases; **1a** > **2a** > **3a** and **1b** > **2b** > **3b**, and 2) small red-shifts were observed when the diimine ligand was changed from dmp to dmpp for all diphosphine complexes. The TD-DFT results reproduce the former trend accurately. As for the second point, the observed and calculated wavelengths are inconsistent. The observed red-shift is small (6-11 nm) therefore we thought more accurate calculations should be necessary. The long-range corrected functional[37] and solvent correction such as PCM model may resolve the problem.

The result of the TDDFT calculation clearly shows that the calculated oscillator strengths of the lowest-energy ^{1}MLCT transitions of the dmpp complexes are about twice of those of the dmp complexes; the calculated oscillator strengths for the lowest-energy transitions of **1a**, **2a**, and **3a** are 0.09, 0.07, and 0.023, respectively, while those for **1b**, **2b**, and **3b** are 0.15, 0.13, and 0.048, respectively. The results also agree with the experimental fact that the absorption coefficients of the lowest-energy bands for **1b**, **2b**, and **3b** are greatly enhanced compared to those for **1a**, **2a**, and **3a**, respectively. Care should be necessary for **3a** and **3b**, because these complexes have two chromophores and the two transitions of opposite direction occur simultaneously, so the calculated oscillator strength should be underestimated. Although the result of the TDDFT study clearly shows the significant effect of the phenyl groups on the electronic transition, the results do not apparently illustrate how the phenyl groups on the phenanthroline ring affect the electronic transitions. Therefore, we use the Multifwn software[30] to analyze the TDDFT results. In the TDDFT method, a large number of combinations of the K-S orbitals, which was obtained in the ground state, are used to calculate the transition moments and energies of the transition. The Multifwn software shows the magnitude of the transition moments for each combination of the K-S orbitals. Analyses of the TDDFT results by the software have shown that the enhancement of the oscillator strength is indicated if only the HOMO → LUMO transition was considered in the TDDFT calculation; for example, the transition dipole strength was calculated as 1.99 (atomic unit) for **1b**, while it was 1.67 for **1a** (Table S2-1a and S2-1b). Oscillator strengths are proportional to the square of the transition moments, therefore the ratio, **1b** vs **1a**, of the calculated oscillator strength for the HOMO → LUMO term is calculated to $(1.99 / 1.67)^2 = 1.42$. Therefor an important result could be drawn by the result; although the contribution of the two phenyl groups in LUMO of **1b** is small (7%), it should enhance the transition dipole moment by 42%. The fact that the distance from the metal center to the phenyl groups is long may be the reason for the considerably large effect. The ratio of the oscillator strengths, **1b** vs. **1a** is calculated to $(1.51 / 1.15)^2 = 1.72$ when all 13561 and 18711 combinations were considered in the TDDFT calculation. therefore the results reasonably account for the fact that the oscillator strength of **1b** was about twice of that of **1a**. The similar results were obtained for **2a** and **2b** (Table S2-2a and S2-2b), and **3a** and **3b** (Table S2-3a and S2-3b).

At the last part of the discussion, we add a brief comment on the intensity of the pure phosphorescence. Even if the major part of the luminescence of the complexes is TADF, a part of the emission should come from pure phosphorescence. There is significant participation of HOMO-3 (HOMO-6 and HOMO-7 for **3a**

and **3b**), in which the phenyl moieties have a considerable contribution in some triplet MLCT excited states as shown in Table 4. This may be related to the increase in the observed radiative decay rates of **1b**, **2b**, and **3b** compared with **1a**, **2a**, and **3a**. It has been reported that the phosphorescent processes of Cu(I)-diimine complexes borrow intensity from the lowest-energy singlet MLCT,[38] so the intense MLCT absorption should increase the radiative rate of the phosphorescence process.

Conclusion

In this study, we prepared the copper(I) complexes bearing diphenyl-substituted phenanthroline ligand, dmpp, and a series of diphosphine ligands, and explored the structures and photophysical properties of the complexes. The two phenyl groups have a marked effect on the photophysical properties of the complexes; the radiative rates of the emissive decay were doubled by the two phenyl groups, on the other hand, essentially no effect on the non-radiative rates. This makes the dmpp complexes very strongly emissive. TDDFT calculation gave an explanation not only for the energy-trend of the complexes, **1b**, **2b**, and **3b**, but also for the dramatic increase in the oscillator strength of the dmpp complexes compared with the dmp complexes; this should affect the increase in the radiative constants of the emitting states.

Acknowledgements

This work was partially supported by Grants-in-Aid from MEXT of Japan (19550070, 26410077), and the Grant from the Faculty of Science and Technology, Seikei University.

References

1. A. Barbieri, G. Accorsi, and N. Armaroli, *Chem. Commun.*, 2008, 2185–2193.
2. S. Sakaki, T. Kuroki, and T. Hamada, *J. Chem. Soc., Dalton Trans.*, 2002, 840–842.
3. T. Bessho, E. C. Constable, M. Graetzel, A. H. Redondo, C. E. Housecroft, W. Kylberg, M. K. Nazeeruddin, M. Neuburger, and S. Schaffner, *Chem. Commun.*, 2008, 3717–3719.
4. Q. Zhao, F. Li, and C. Huang, *Chem. Soc. Rev.*, 2010, **39**, 3007–3030.
5. C. S. Smith, C. W. Branham, B. J. Marquardt, and K. R. Mann, *J. Am. Chem. Soc.*, 2010, **132**, 14079–14085.
6. O. Horváth, *Coord. Chem. Rev.*, 1994, **135–136**, 303–324.
7. N. Armaroli, G. Accorsi, F. Cardinali, and A. Listorti, in *Photochemistry and Photophysics of Coordination Compounds I*, eds. V. Balzani and S. Campagna, Springer Berlin Heidelberg, 2007, pp. 69–115.
8. S. B. Harkins and J. C. Peters, *J. Am. Chem. Soc.*, 2005, **127**, 2030–2031.
9. A. J. M. Miller, J. L. Dempsey, and J. C. Peters, *Inorg. Chem.*, 2007, **46**, 7244–7246.
10. M. J. Leitl, F.-R. Küchle, H. A. Mayer, L. Wesemann, and H. Yersin, *J. Phys. Chem. A*, 2013, **117**, 11823–11836.
11. A. Tsuboyama, K. Kuge, M. Furugori, S. Okada, M. Hoshino, and K. Ueno, *Inorg. Chem.*, 2007, **46**, 1992–2001.
12. T. Tsubomura, N. Takahashi, K. Saito, and T. Tsukuda, *Chem. Lett.*, 2004, **33**, 678–679.

13. T. Tsukuda, A. Nakamura, T. Arai, and T. Tsubomura, *Bull. Chem. Soc. Jpn.*, 2006, **79**, 288–290.
14. K. Matsumoto, N. Matsumoto, A. Ishii, T. Tsukuda, M. Hasegawa, and T. Tsubomura, *Dalton Trans.*, 2009, 6795.
15. V. A. Krylova, P. I. Djurovich, B. L. Conley, R. Haiges, M. T. Whited, T. J. Williams, and M. E. Thompson, *Chem. Commun.*, 2014, **50**, 7176.
16. R. Czerwieniec, J. Yu, and H. Yersin, *Inorg Chem*, 2011, **50**, 8293–8301.
17. L. Bergmann, J. Friedrichs, M. Mydlak, T. Baumann, M. Nieger, and S. Bräse, *Chem. Commun.*, 2013, **49**, 6501–6503.
18. L.-Y. Zou, Y.-X. Cheng, Y. Li, H. Li, H.-X. Zhang, and A.-M. Ren, *Dalton Trans.*, 2014, **43**, 11252.
19. K. Saito, T. Arai, N. Takahashi, T. Tsukuda, and T. Tsubomura, *Dalton Trans.*, 2006, 4444–4448.
20. N. Armaroli, G. Accorsi, M. Holler, O. Moudam, J.-F. Nierengarten, Z. Zhou, R. T. Wegh, and R. Welter, *Adv. Mater.*, 2006, **18**, 1313–1316.
21. Z. Xu, C. Xu, Q. Wang, W. Jiang, C. Liu, L. Liu, M. Liu, W. Li, G. Che, and F. Shi, *Synthetic Metals*, 2010, **160**, 2260–2264.
22. G. J. Kubas, *Inorg. Synth.*, 1979, **19**, 90–92.
23. H. Uesugi, T. Tsukuda, K. Takao, and T. Tsubomura, *Dalton Trans.*, 2013, **42**, 7396–7403.
24. K. Suzuki, A. Kobayashi, S. Kaneko, K. Takehira, T. Yoshihara, H. Ishida, Y. Shiina, S. Oishi, and S. Tobita, *Phys. Chem. Chem. Phys.*, 2009, **11**, 9850.
25. (a) Rigaku Corporation, *CrystalClear.* Rigaku Corporation, Tokyo, Japan. (b) M. C. Burla, R. Caliandro, M. Camalli, B. Carrozzini, G. L. Cascarano, L. De Caro, C. Giacovazzo, G. Polidori and R. Spagna, *J. Appl. Crystallogr.*, 2005, **38**, 381-388. (c) A. Altomare, G. Cascarano, C. Giacovazzo, A. Guagliardi, M. C. Burla, G. Polidori and M. Camalli, *J. Appl. Crystallogr.*, 1994, 27, 435–436. (d) G. M. Sheldrick, *Acta Crystallogr., Sect. A: Fundam. Crystallogr.,* 2007, 64, 112–122. (e) Rigaku Corporation, *CrystalStructure*, Tokyo, Japan. (f) Farrugia, L. J. *J. Appl. Cryst.* 1999, 32, 837–838. (f) P. van der Sluis and A. L. Spek, *Acta Crystallogr., Sect. A: Fundam. Crystallogr.*, 1990, **46**, 194–201.
26. M. J. Frisch, G. W. Trucks, H. B. Schlegel, G. E. Scuseria, M. A. Robb, J. R. Cheeseman, J. A. Montgomery, Jr., T. Vreven, K. N. Kudin, J. C. Burant, J. M. Millam, S. S. Iyengar, J. Tomasi, V. Barone, B. Mennucci, M. Cossi, G. Scalmani, N. Rega, G. A. Petersson, H. Nakatsuji, M. Hada, M. Ehara, K. Toyota, R. Fukuda, J. Hasegawa, M. Ishida, T. Nakajima, Y. Honda, O. Kitao, H. Nakai, M. Klene, X. Li, J. E. Knox, H. P. Hratchian, J. B. Cross, V. Bakken, C. Adamo, J. Jaramillo, R. Gomperts, R. E. Stratmann, O. Yazyev, A. J. Austin, R. Cammi, C. Pomelli, J. W. Ochterski, P. Y. Ayala, K. Morokuma, G. A. Voth, P. Salvador, J. J. Dannenberg, V. G. Zakrzewski, S. Dapprich, A. D. Daniels, M. C. Strain, O. Farkas, D. K. Malick, A. D. Rabuck, K. Raghavachari, J. B. Foresman, J. V. Ortiz, Q. Cui, A. G. Baboul, S. Clifford, J. Cioslowski, B. B. Stefanov, G. Liu, A. Liashenko, P. Piskorz, I. Komaromi, R. L. Martin, D. J. Fox, T. Keith, M. A. Al-Laham, C. Y. Peng, A. Nanayakkara, M. Challacombe, P. M. W. Gill, B. Johnson, W. Chen, M. W. Wong, C. Gonzalez, and J. A. Pople, *Gaussian 03, Revision E.01*, Gaussian, Inc., Wallingford, CT, 2007.
27. A. J. H. Wachters, *J. Chem. Phys.*, 1970, **52**, 1033–1036.
28. U. Varetto, *Molekel*, Swiss National Supercomputing Centre: Lugano, Switzerland.
29. S. I. Gorelsky, *AOMix: Program for Molecular Orbital Analysis*, University of Ottawa, 2011.
30. T. Lu and F. Chen, *J. Comput. Chem.*, 2012, **33**, 580–592.
31. S.-M. Kuang, D. G. Cuttell, D. R. McMillin, P. E. Fanwick, and R. A. Walton, *Inorg. Chem.*, 2002, **41**, 3313–3322.
32. A. Kaeser, M. Mohankumar, J. Mohanraj, F. Monti, M. Holler, J.-J. Cid, O. Moudam, I. Nierengarten, L. Karmazin-Brelot, C. Duhayon, B. Delavaux-Nicot, N. Armaroli, and J.-F. Nierengarten, *Inorg. Chem.*, 2013, **52**, 12140–12151.

33. J. R. Kirchhoff, R. E. Gamache, M. W. Blaskie, A. A. Del Paggio, R. K. Lengel, and D. R. McMillin, *Inorg. Chem.*, 1983, **22**, 2380–2384.
34. D. R. McMillin and K. M. McNett, *Chem. Rev.*, 1998, **98**, 1201–1220.
35. Some k_r values of the previous paper should be wrong. Calculation ($k_r = \Phi / \tau$) shows that the k_r values of **2a** and **3a** are 0.68 (0.76)$\times 10^4$ s^{-1} and 0.92 (1.1) $\times 10^5$ s^{-1}. The previous values reported in ref. 19 are shown in parentheses.
36. (a) R. Czerwieniec, K. Kowalski, and H. Yersin, *Dalton Trans.*, 2013, **42**, 9826-9830. (b) M. Nishikawa, S. Sawamura, A. Haraguchi, J. Morikubo, K. Takao and T. Tsubomura, *Dalton Trans.* 2014, **44**, 411- 418.
37. Y. Tawada, T. Tsuneda, S. Yanagisawa, T. Yanai, and K. Hirao, *J. Chem. Phys.*, 2004, **120**, 8425-8433.
38. Z. A. Siddique, Y. Yamamoto, T. Ohno, and K. Nozaki, *Inorg. Chem.*, 2003, **42**, 6366–6378.

Table 1 Selected bond lengths and angles for the copper(I) complexes.

	1b	**2b**	**3b**
Cu1 – N1	2.056(2)	2.050(3)	2.080(4)
Cu1 – N2	2.024(2)	2.068(3)	2.130(4)
Cu1 – P1	2.2403(6)	2.2322(10)	2.2669(15)
Cu1 – P2	2.2464(7)	2.2396(9)	2.2915(16)
N1 – Cu1 – N2	81.74(8)	81.46(11)	80.03(14)
P1 – Cu1 – P2	90.70(2)	104.92(4)	119.57(5)
α[a]	85.5	87.5	89.0
β_1, β_2[b]	58.4, 51.6	64.3, 55.1	59.2, 49.9

a) The dihedral angles specified by the two planes, which are determined by the coordinates of Cu1, N1 and N2 atoms and Cu1, P1 and P2 atoms, respectively. b) The dihedral angles between the mean plane of phenanthroline ring and the phenyl group on the N1 and N2 side, respectively.

Table 2 Photophysical data for the copper(I) complexes.

complex	**1a**[a]	**1b**	**2a**[b]	**2b**	**3a**[b]	**3b**
diimine ligand	dmp	dmpp	dmp	dmpp	dmp	dmpp
diphosphine ligand	dppe		dppp		dppb	
λ_{abs} / nm	400	411	391	402	382	388
ε / $mol^{-1}dm^3cm^{-1}$	3200	6200	3200	5900	2800[c]	5000[c]
λ_{em} / nm	630	627	600	608	590	585
Φ	0.010	0.017	0.037	0.066	0.10	0.16
τ / μs	1.3	1.2	5.4	4.4	10.8	10.0

[a] Reference [31] [b] Reference [19]. [c] The molar extinction coefficients were calculated using a half of the molecular weight of the dinuclear complexes.

The quantum yield for $[Cu(dmp)(dppe)]^+$ was reported to 0.01 based on the standard value (Φ 0.042 for $[Ru(bpy)_3]^{2+}$ in deoxygenated water).[32] If the recently reported value of 0.063 (Reference 24) is employed for the standard, the value for $[Cu(dmp)(dppe)]^+$ should be 0.015. In this case, k_r and k_{nr} of $[Cu(dmp)(dppe)]^+$ are calculated to be 1.1×10^4 s^{-1} and 7.4×10^5 s^{-1}, respectively. Even if these values are correct, the conclusion of the discussion did not change.

Table 3. The results of the Mulliken population analysis for the DFT results of the structure-optimization for the copper(I) complexes. The "components" shown in the table is the components ratio of the K-S orbitals; P-P, N-N, Ph2 represent diphosphine ligand, phenanthroline ligand and diphenyl moiety respectively. For the complexes 1b, 2b, and 3b, N-N denotes dimethylphenanthroline ligand except the two phenyl groups.

complex	K-S orbital	energy /eV	components (%) Cu	P-P	N-N	complex	K-S orbital	energy /eV	components (%) Cu	P-P	N-N	Ph2
	LUMO+2	-3.05	5	97	-2		LUMO+2	-2.93	4	97	-1	0
	LUMO+1	-4.20	0	0	100		LUMO+1	-4.02	0	0	90	9
	LUMO	-4.40	3	2	96		LUMO	-4.19	3	2	88	7
1a	HOMO	-7.74	55	39	6	**1b**	HOMO	-7.56	52	37	8	2
	HOMO-1	-8.36	73	7	20		HOMO-1	-8.14	71	7	21	1
	HOMO-2	-8.62	71	21	7		HOMO-2	-8.45	47	13	27	12
	HOMO-3	-8.99	1	18	82		HOMO-3	-8.49	31	10	38	20
	LUMO+2	-3.02	4	13	83		LUMO+2	-2.90	2	33	56	9
	LUMO+1	-4.21	0	0	99		LUMO+1	-4.04	0	0	89	10
	LUMO	-4.40	2	2	96		LUMO	-4.20	2	2	88	8
2a	HOMO	-7.81	56	37	6	**2b**	HOMO	-7.62	54	35	9	3
	HOMO-1	-8.31	74	9	16		HOMO-1	-8.09	74	7	18	0
	HOMO-2	-8.48	73	19	8		HOMO-2	-8.32	73	18	9	0
	HOMO-3	-8.96	8	72	21		HOMO-3	-8.48	6	6	57	31
	LUMO+5	-4.33	3	92	5		LUMO+5	-4.14	2	93	4	0
	LUMO+4	-4.35	4	90	5		LUMO+4	-4.16	4	91	5	0
	LUMO+3	-5.32	0	1	99		LUMO+3	-5.05	1	1	90	9
	LUMO+2	-5.32	0	1	99		LUMO+2	-5.05	0	1	90	9
	LUMO+1	-5.56	2	1	97		LUMO+1	-5.27	2	1	89	8
	LUMO	-5.57	2	1	97		LUMO	-5.28	2	1	89	8
3a	HOMO	-9.26	56	36	8	**3b**	HOMO	-8.96	49	30	15	6
	HOMO-1	-9.26	57	35	8		HOMO-1	-8.96	50	29	15	6
	HOMO-2	-9.52	71	16	13		HOMO-2	-9.22	77	6	17	1
	HOMO-3	-9.53	77	9	15		HOMO-3	-9.22	78	4	17	1
	HOMO-4	-9.56	80	10	9		HOMO-4	-9.32	73	19	7	1
	HOMO-5	-9.59	78	15	7		HOMO-5	-9.35	74	17	8	1
	HOMO-6	-10.10	2	19	79		HOMO-6	-9.50	12	10	42	37
	HOMO-7	-10.10	2	17	80		HOMO-7	-9.50	11	9	42	37

Table 4 TDDFT results. Calculated transition wavelength, oscillator strength (*f*), components of singlet add triplet excited states are shown. The calculations were performed based on the optimized geometry in the ground states. Two major components are shown for each transition.

	singlet				triplet		
complex	λ / nm	*f*	components and coefficients		λ / nm	components and coefficients	
1a	451	0.09	HOMO → LUMO	0.68	499	HOMO → LUMO	0.70
	422	0.017	HOMO → LUMO+1	0.69	470	HOMO-1→ LUMO+1	0.58
						HOMO-3 → LUMO+1	-0.40
1b	446	0.15	HOMO → LUMO	0.68	496	HOMO → LUMO	0.70
						HOMO-3 → LUMO	-0.10
	419	0.05	HOMO → LUMO+1	0.69	483	HOMO → LUMO+1	0.55
						HOMO-3 → LUMO+1	-0.31
2a	443	0.07	HOMO → LUMO	0.68	486	HOMO → LUMO	0.70
	419	0.0006	HOMO-1 → LUMO	0.68	465	HOMO → LUMO+1	0.56
			HOMO-2 → LUMO	-0.12		HOMO-5→ LUMO+1	-0.38
2b	438	0.13	HOMO → LUMO	0.68	487	HOMO → LUMO	0.69
						HOMO-3 → LUMO	-0.15
	417	0.0008	HOMO-1 → LUMO	0.69	481	HOMO → LUMO+1	0.54
						HOMO-3 → LUMO+1	-0.41
3a	410	0.023	HOMO-3 → LUMO	0.42	456	HOMO → LUMO	0.38
			HOMO-2 → LUMO+1	0.37		HOMO-1 → LUMO+1	0.38
			HOMO → LUMO	-0.25	456	HOMO-1 → LUMO	0.38
			HOMO-1 → LUMO+1	-0.25		HOMO → LUMO+1	0.38
	403	0.095	HOMO-1 → LUMO+1	0.042			
			HOMO → LUMO	0.42			
3b	408	0.048	HOMO-3 → LUMO	0.42	472	HOMO → LUMO	0.34
			HOMO-2 → LUMO+1	0.42		HOMO-1 → LUMO+1	0.34
			HOMO → LUMO	-0.25		HOMO-1 → LUMO+3	-0.20
			HOMO-1 → LUMO+1	-0.25		HOMO-7 → LUMO+3	-0.20
	401	0.23	HOMO → LUMO	0.42		HOMO-6 → LUMO+2	-0.20
			HOMO-1 → LUMO+1	0.42		HOMO→ LUMO+2	-0.20
			HOMO-3 → LUMO	0.25	472	HOMO-1 → LUMO	0.34
			HOMO-2 → LUMO+1	0.25		HOMO → LUMO+1	0.34
						HOMO → LUMO+3	-0.20
						HOMO-6 → LUMO+3	-0.20
						HOMO-7 → LUMO+2	-0.20
						HOMO-1 → LUMO+2	-0.20

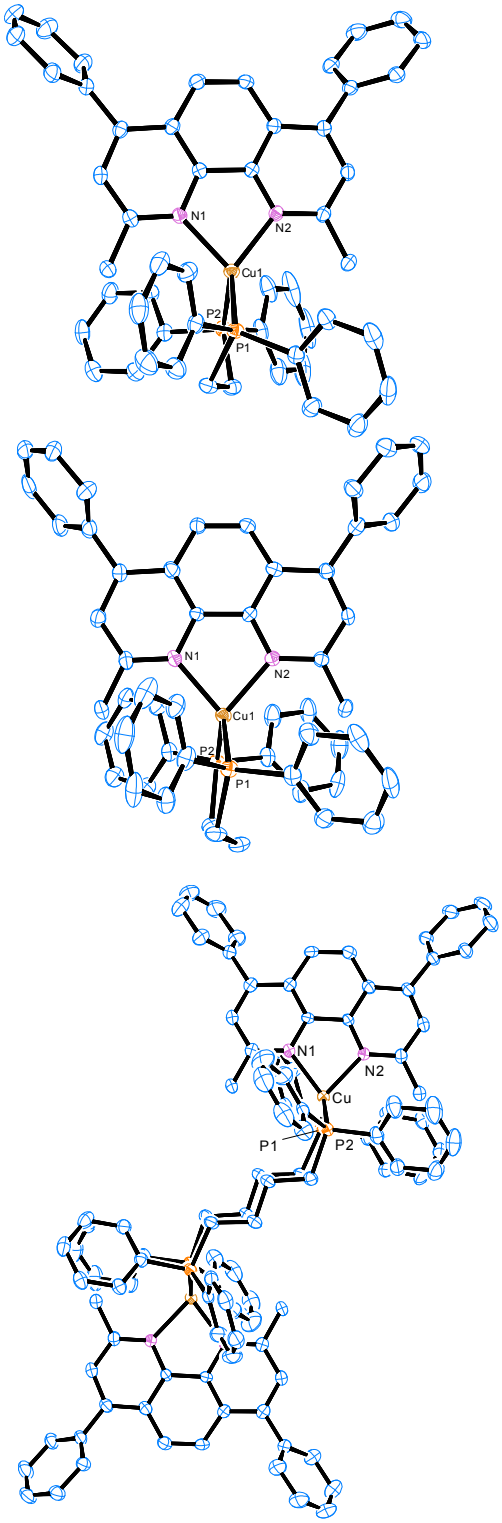

Fig. 1 ORTEP drawings of **1b** (top), **2b** (middle), and **3b** (bottom). Thermal ellipsoids were drawn with 30% probability.

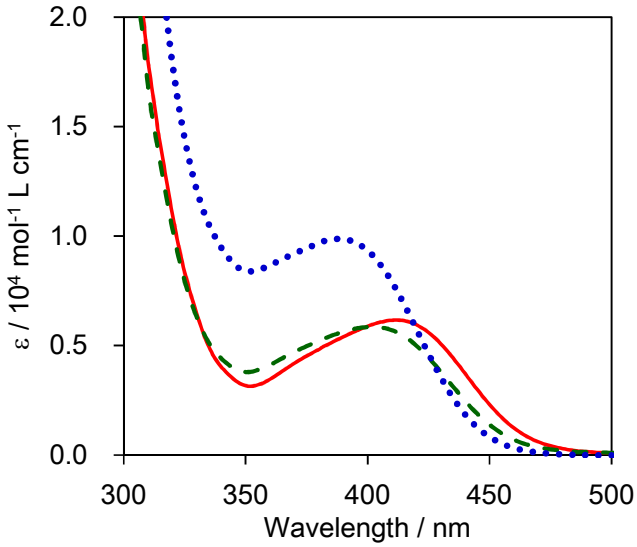

Fig. 2 Absorption spectra of **1b** (red, solid line), **2b** (green, dashed line), and **3b** (blue, dotted line) in dichloromethane solution at room temperature.

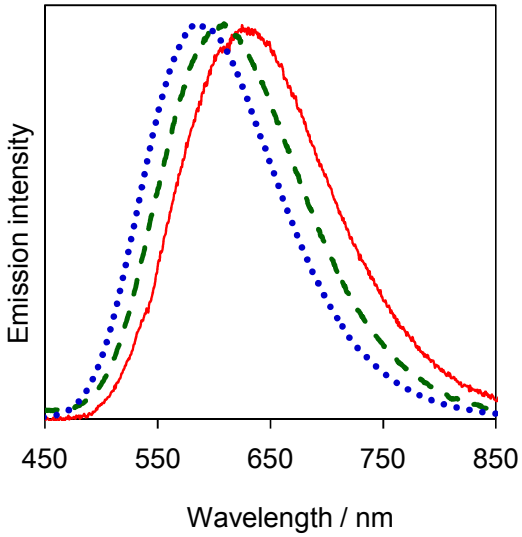

Fig. 3 Emission spectra of **1b** (red, solid line), **2b** (green, dashed line), and **3b** (blue, dotted line) in dichloromethane solution at room temperature. Emission intensity was not corrected for wavelength dependence.

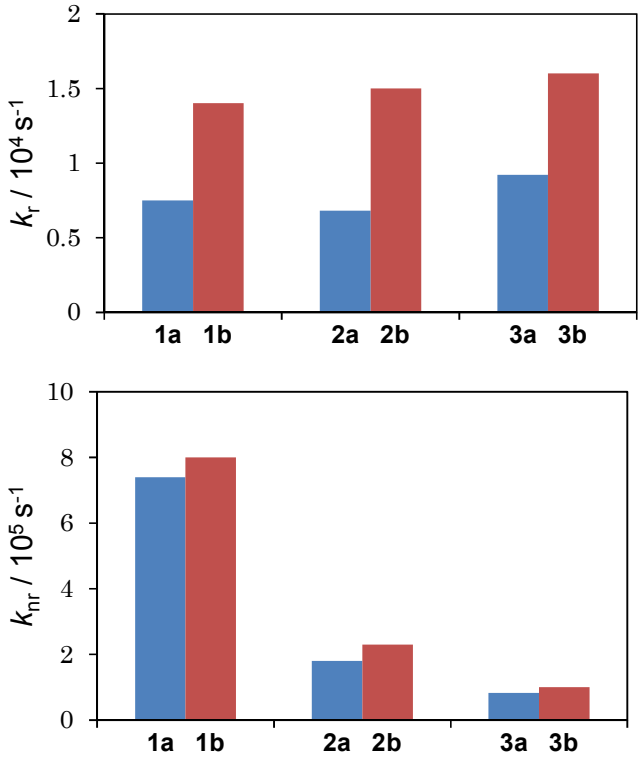

Fig. 4 The comparison of the observed radiative rate constants k_r and the observed non-radiative rate constants k_{nr}.

Structures and Photophysical Properties of Copper(I) Complexes Bearing Diphenylphenanthroline and Bis(diphenylphosphino)alkane: The Effect of Phenyl Groups on the Phenanthroline Ligand

Taro Tsubomura, Kaoru Kimura, Michihiro Nishikawa, and Toshiaki Tsukuda

TOC graphic

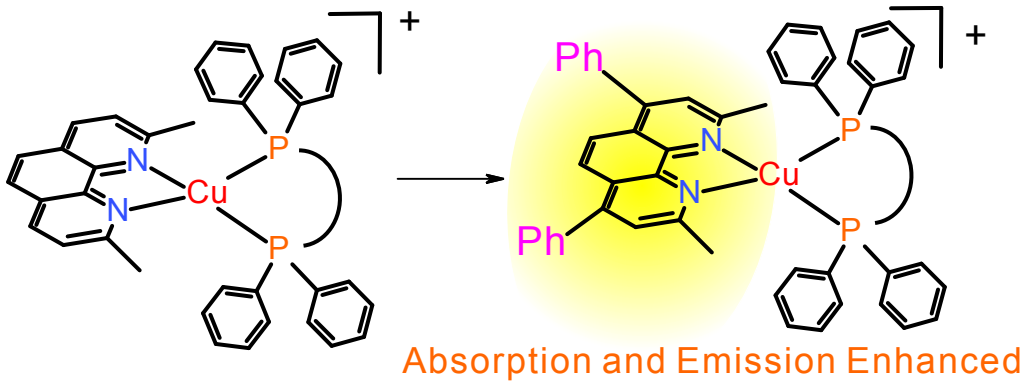

Emissive copper(I) complexes bearing a phenanthroline ligand having diphenyl groups and a diphosphines were synthesized. The quantum yields are enhanced by the diphenyl groups on the phenanthroline ligand.